DIRECT PCR AMPLIFICATION AND IN SITU IMAGING BASED ON ALGINATE DROPLETS

Lijun Li[1], Linfen Yu[1], and Tianzhun Wu[1]**

[1]Shenzhen institute of Advanced Technology, Chinese Academy of Science, Shenzhen, China

ABSTRACT

A droplet based microfluidic system encapsulating PCR reagent into alginate beads as a new digital PCR solution has been developed, which avoided droplet coalescence and enabled efficient DNA amplification and high-throughput fluorescent imaging. We also compared two trapping methods using hydrodynamic traps and micro-sieves, and indicated the advantages of latter for higher trapping rate and no droplet clogging. These results provide new insights and tools for on-chip digital PCR and are expected to attract broad interest for applications in droplet microfluidics.

INTRODUCTION

Polymerase chain reaction (PCR) was invented over three decades ago by Kary Mullis[1], which has become very popular for biology due to its high efficiency and easy access to amplify nucleic acid. Fluorescent dyes was introduced into the reaction mixture[2] to facilitate real-time monitoring. This improvement of this method resulted in the relative quantification of initial copies of DNA based on standard curves, known as qPCR. The third generation PCR, i.e., digital PCR (dPCR), enables absolutely quantitative assay[3] without using bulk solution. In dPCR technology the sample solution is divided into thousands or more sub-samples, and each of them contains no more than one molecule of DNA ("0" or "1") on average. The molecule distribution obeys the Poisson distribution as following:

$$\lambda = -\ln(1-p), \qquad (1)$$

where p is the fraction of positive droplets and λ represents target copies per droplet. The number of molecules in the initial sample can be calculated from the fraction of positive end-point reactions[4]. dPCR has the advantages such as absolute quantification[5], higher sensitivity[6] and selectivity[7]. Furthermore, digital PCR offers the unique solution for samples with minor differences in starting molecule count or rare target DNAs[8]. Microfluidics offers several options for the precise partition of small-volume samples, either by creating sequence of droplets or microwells[9]. For example, by segregating single DNA molecules in individual water-in-oil emulsion droplets, dPCR demonstrated massively parallel clonal amplification of DNA templates, which allows the identification and quantification of rare mutant gene within a large population [10, 11], and enables new generation of high-throughput DNA sequencing technologies [12]. It can also prevent crossover contamination and PCR inhibition [13], promising for single-cell and single-molecule analysis.

Although various dPCR chips have been developed and commercialized, there are only limited reports which integrated droplet formation, PCR amplification, and fluorescent signal detection into one chip, which is highly preferred to improve efficiency. Bian *et al.* demonstrated the simultaneous and sensitive detection of pathogenic Escherichia coli O157 and Listeria monocytogenes using a duplex droplet digital PCR platform. The platform, which used a mineral oil saturated polydimethylsiloxane (OSP) chip to overcome the problem of droplet evaporation, integrated the functions of droplet generation, on-chip amplification and end-point fluorescence readout. Compared with a quantitative real-time PCR approach, the OSP chip-based duplex dPCR platform exhibited high sensitivity, which is at the level of single molecule resolution without significant cross-assay interference. This integrated system was also used to analysis lung cancer related microRNA[15], however, the manufacture of the OSP chip is not easy and is time-consuming[14].

An ideal microfluidic system with integrated on-chip PCR should be fully autonomous, easy for non-experts to use. To achieve these, there are still some problems, such as droplet coalescence and clogging, leading to wrong results based on Poisson distribution. Here we try to solve this question by introducing alginate to the integrated dPCR system for producing stable droplet beads without clogging. Alginate is a linear polysaccharide comprised of combinations of β-D-mannuronic and α-L-guluronic acid residues, works as an exceptional polymer for many encapsulation purposes due to its biocompatibility and mild ionic gelation conditions[16]. Introducing alginate also open the possibility for more potential utilization, such as encapsulating cells or other biological molecules.

To address the existing issue of single-chip integration and droplet coalescence, in this paper, we developed a high-throughput technology enabling formation and encapsulating the PCR sample into solid alginate beads, and immobilizing beads in individual chambers, which facilitated the single-chip PCR amplification and fluorescent imaging. We also compared two trapping methods using hydrodynamic traps and micro-sieves, and indicated the advantages of latter for higher trapping rate and avoiding droplet clogging.

METHODS AND MATERIALS

Droplet formation using alginate

The microfluidic chips were fabricated in poly-dimethylsiloxane (PDMS, Sylgard 184, Dow Corning, USA) using the standard soft lithographic techniques[23]. High aspect ratio features were first patterned using SU-8 3050 (MicroChem Corporation, USA) photoresist on a silicon substrate using a mask aligner (EVG 610, Austria). These features later defined the microchannels and

inlet/outlet reservoirs. The SU-8 on the silicon wafer served as the mold master, onto which PDMS was poured. PDMS was cured at 80 ℃ for 1 h, then was peeled off from the mold master. The PDMS channel was bonded to a glass substrate on which a thin layer of PDMS was spin-coated and cured, so that all four interior walls of the microfluidic channel would have the same surface properties. To avoid adsorption, the microfluidic channels were coated by parylene-C vapor deposition with the thickness of 2 μm (SCS Coatings, USA).

The schematic of the droplet-based microfluidic device is shown in Fig. 1a. The alginate encapsulated PCR droplet was formed on the microfluidic chip using multiple inlet flows in a flow focusing geometry. The water dispersed phase (1) consisted of alginate precursor, PCR reagent, insoluble calcium carbonate particles, potassium chloride and sodium chloride dispersed in solution. The immiscible continuous phase (2) was mineral oil containing 2 μL/mL acetic acid and 2.5% surfactant Span 80 (Sigma-Aldrich Co.). The outlet of chip flows to the collection vial, where gel beads were collected. The alginate powder (Sigma-Aldrich Co. A2033) was dissolved in sterile water and stirred overnight. Powder of $CaCO_3$ particles (J.T. Baker@1301-01) was dissolved and sonicated in sterile water at the concentration of 2 M. The final concentration of $CaCO_3$ in alginate solution was 40 mM, and the final concentration of potassium chloride and sodium chloride is respectively 7 mM and 75 mM. Alginate gels via calcium-mediated crosslinking. Calcium, bound in the insoluble form of $CaCO_3$, is mixed into an ungelled alginate solution of high or neutral pH. When the pH is lowered, the acid reacts with the calcium carbonate to release water, CO_2 and Ca^{2+}, initiating alginate gelation. Na^+ and K^+ avoid the inhibition of alginate to PCR amplification. Here, the oil phase is acidified, and as the alginate droplets spend more time in the oil, more acid will diffuse into the alginate, causing Ca^{2+} release and alginate gelation. Once gelled, the beads can be collected in a parallel of trapping chambers, which can be located for downstream PCR amplification and fluorescent imaging analysis.

Droplet trapping

We designed two structures for trapping beads shown in Fig. 2 and Fig. 3. For the first one using the hydrodynamic traps[17], droplets were captured and immobilized following the path of microwells with minimum flow resistance. Here, the droplets were captured and immobilized to follow the path with smaller flow resistance along the microchannels. Figure 2 illustrates the principle of the droplet trapping process. The successive generated droplets are numbered sequentially. The serial paths from junction I , II to N are named as Path 1 and Path 2, …and Path N, and the flow resistances along them are defined as R1, R2 to RN. The process for trapping one droplet is described as follows: (a) R1 > R2, droplet 1 at junction I will flow into Path 2; (b) R2 > R1, droplet 2 at junction I will flow into Path 1 and be trapped; (c) R1 > R2, droplet 3 at junction I will flow into Path 2 and enter the next trapping process. For the second one, a continuous and orthogonal flow based on the micro-sieve structure was found to avoid the clogging issue. Beads were generated and moved horizontally from left to right, and simultaneously a constant vertical pressure was applied to drive beads to travel diagonally into the micro-sieves for trapping. We designed a high-throughput droplet trapping matrix as shown in Fig 3. There are totally 62 parallel rows with 95 U-shaped microsieves in each row. Each micro-sieve is semicircular with a 20 um apertures.

Droplet PCR and Imaging

We designed an integrated chip and further investigated the capability of this system for encapsulation of alginate beads carrying PCR reagent, and applied it for H7N9 amplification and image. A reverse transcription PCR (RT-PCR) thermocycler used cycling protocol: a reverse transcription step at 42 ℃ for 25 minutes, and then an initial denaturation step at 95 ℃ for 3 minutes, 40 cycles of denaturation (95 ℃ for 8 s), annealing and extension (60 ℃ for 35 s), and a final step hold on 4 ℃. After RT-PCR we photographed fluorescent image.

RESULTS AND DISCUSSIONS

Droplet formation using alginate

Microfluidic flow focusing produces alginate beads with good size uniformity. The hydrogel alginate beads exhibited a narrow size distribution with CV of 0.08 (Fig. 1b). The average alginate bead diameter was 84.53 μm (equivalently 0.32 nL). The alginate bead structure assists in maintaining spherical droplet and bead shape. And the alginate droplet did not coalesce even when they were strongly squeezed together (Fig. 4a). This simple method of generating alginate droplet beads uses single-layer microfluidic chips with uniform channel height. These chips are readily fabricated using only one photolithography step per channel height.

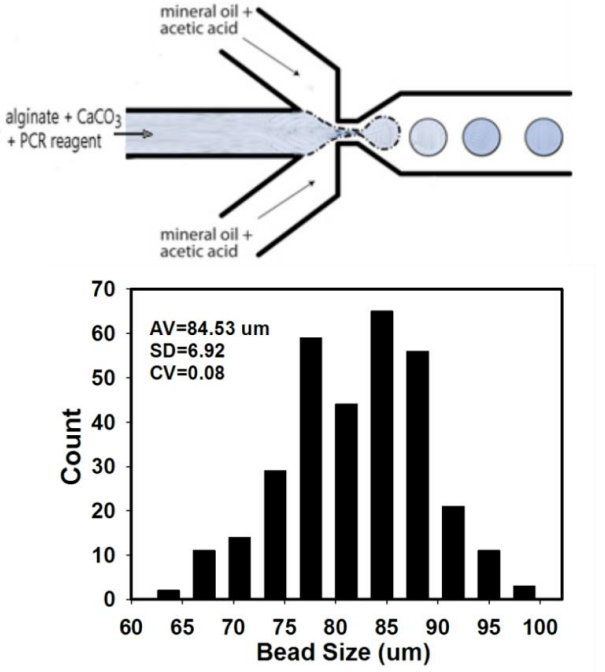

Figure 1: (a) Formation of alginate droplet beads based on flow focusing. (b) The alginate bead size distribution of the alginate beads.CV=8%.

The formation of droplet was related to the concentration of surfactant added into the oil and we tried different concentration of Span 80. We found that the concentration either too low or too highwas disadvantageous for droplet formation and 2.5%(v/v) was the optimal concentration, which was adopted in this paper.

Droplet trapping

The first method based on the hydrodynamic trap (Fig. 2) can trap multiple beads, however, due to the large flow resistance of the long, narrow main channel, droplets easily clogged in the downstream, and significantly reduced the trapping rate. On contrary, the other method (Fig.3) based on micro-sieves had the network of channels which greatly reduced the pressure loss, hence enabled higher capture efficiency for beads. To increase the throughput of trapping efficiency and reduce the clogging issue, we utilized a continuous and orthogonal flow based on the microseives structure. With the continuous flow, each micro-sieve will efficiently retain an alginate bead and achieve an 86.15 % (1950 alginate beads counted) of trapping rate. Therefore micro-sieves microchip achieved high capture efficiency for beads. Figure 4(b,c) showed the beads captured using these two methods. It illustrated that the droplet beads was more uniform trapped by the micro-sieves than that by hydrodynamic traps. There are large flow resistance in the hydrodynamic trap chip, as a result, droplets easily clogged in the downstream. This leads to low trapping rate. To address this problem, the channels have to be designed to be much shorter and wider which does not meet the practical requirement of high-density droplet array.

Droplet PCR and Imaging

Figure 5a exhibited fluorescent microscope image of alginate beads after amplification from H7N9 template. The PCR amplification occurred within the alginate beads.

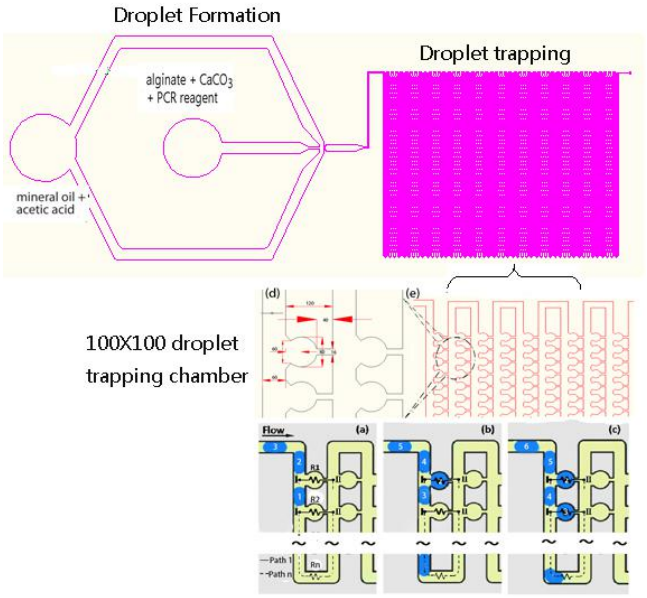

Figure 2: Principle of the droplets captured in the hydrodynamic traps trap array[17].

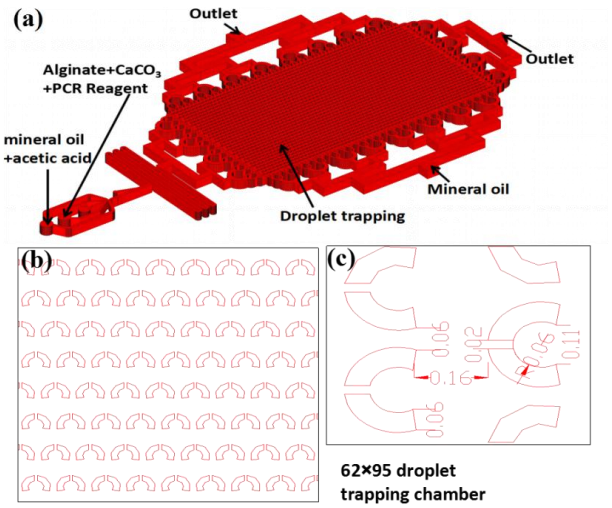

Figure 3: (a) Illustration of a chip with micro-sieves. (b) Illustration of the micro-sieve structure for trapping beads. (c) Dimensions of the micro-sieve structure

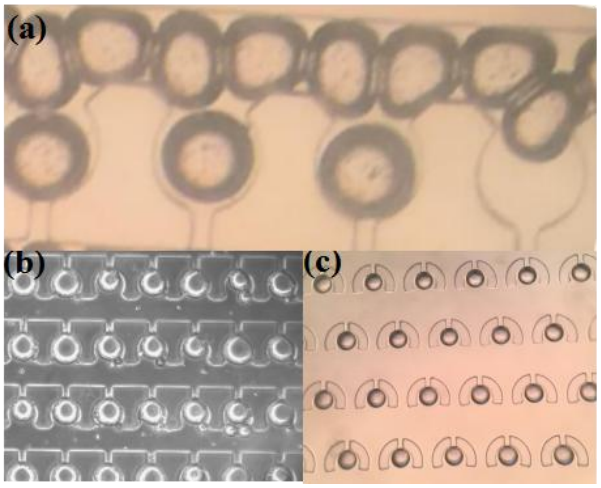

Figure 4: (a)The alginate droplets did not coalesce when they were strongly squeezed together.(b) Image of 100×100 array droplets encapsulated into the individual chambers (hydrodynamic traps). (c) One microscopic image of 62×95 array droplets encapsulated into the micro-sieves.

For the reverse transcription PCR thermocycle, we used the following cycling protocol: a reverse transcription step at 42 ℃ for 25 minutes, then an initial denaturation step at 95 ℃ for 3 minutes, 40 cycles of denaturation (95 ℃ for 8 s), and finally annealing and extension (60 ℃ for 35 s). After RT-PCR the fluorescent microscope image (Fig. 5a) showed that adding alginate did not affect the amplification process. The product comparison of alginate PCR and empty sample using a 1.5% w/v agarose gel was shown in Fig. 5b, which demonstrated the typical DNA amplification in the alginate beads. We anticipate the integrated and automatic system based on the novel solid droplet arrays and the micro-sieve trapping strategy will be of great interest for applications such as gene diagnosis, single-cell analysis and prognosis.

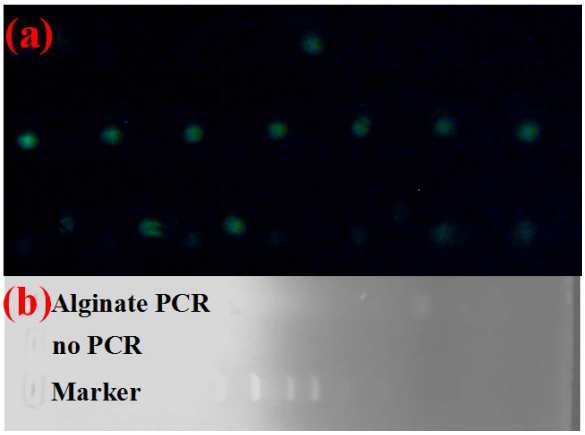

Figure 5: (a) Fluorescent microscope image of alginate beads after amplification from the H7N9 template. (b) The results of alginate PCR product with a 1% w/v agarose gel.

CONCLUSIONS

This droplet based microfluidic system integrating a droplet formation and a droplet trap array is described for encapsulating PCR reagent into a parallel series of alginate beads. The concept of using alginate microspheres as nanoliter-scale reactors for PCR may inspire better approaches for highly efficient DNA amplification and high throughput fluorescent imaging. This platform has the benefit of scaling of dimensions that enables controlled and precise droplet generation and rapid trapping beads into individual chambers, on-chip PCR amplification and fluorescent imaging, which make it a promising and ideal platform for many biological applications, especially for single cell genetic analysis.

ACKNOWLEDGEMENTS

This work is supported by NSFC (No. 51475451), Guangdong Innovative and Entrepreneurial Research Team Program (No. 2013S046), Guangdong Science and Technology Research Program(2015A050502040 ， 2015B020227002)， Shenzhen Science and Technology Research Program (GJHZ20150316143625432) and Shenzhen Peacock Plan .

REFERENCES

[1] Mullis K, Faloona F, Scharf S, et al. Specific Enzymatic Amplification of DNA In Vitro: The Polymerase Chain Reaction[J]. Cold Spring Harbor Symposia on Quantitative Biology, 1986, 51 Pt 1(1):263-73.

[2] Chehab F F. Detection of specific DNA sequences by fluorescence amplification: a color complementation assay.[J]. Proceedings of the National Academy of Sciences of the United States of America, 1989, 86(23):9178-82.

[3] Vogelstein B, Kinzler K W. Digital Pcr[J]. Proceedings of the National Academy of Sciences of the United States of America, 1999, 96(16):9236-41.

[4]Wang J, Ramakrishnan R, Tang Z, et al. Quantifying EGFR Alterations in the Lung Cancer Genome with Nanofluidic Digital PCR Arrays[J]. Clinical Chemistry, 2010, 56(4):623-32.

[5]Yung T K F, Chan K C A, Mok T S K, et al. Single-molecule detection of epidermal growth factor receptor mutations in plasma by microfluidics digital PCR in non-small cell lung cancer patients.[J]. Clinical Cancer Research, 2009, 15(6):2076-84.

[6]Ottesen E A, Hong J W, Quake S R, et al. Microfluidic digital PCR enables multigene analysis of individual environmental bacteria.[J]. Science, 2006, 314(5804):1464-7.

[7]Strain M C, Lada S M, Luong T, et al. Highly precise measurement of HIV DNA by droplet digital PCR[J]. Plos One, 2013, 8(4):e55943.

[8]Hindson B J, Ness K D, Masquelier D A, et al. High-throughput droplet digital PCR system for absolute quantitation of DNA copy number.[J]. Analytical Chemistry, 2011, 83(22):8604-10.

[9]Pompano R R, Liu W, Du W, et al. Microfluidics Using Spatially Defined Arrays of Droplets in One, Two, and Three Dimensions[J]. Annual Review of Analytical Chemistry, 2011, 4(1):59-81.

[10]Pekin D, Skhiri Y, Baret J C, et al. Quantitative and sensitive detection of rare mutations using droplet-based microfluidics.[J]. Lab on A Chip, 2011, 11(13):2156-66.

[11] Zhang Y, Jiang H R. A Review on Continuous-Flow Microfluidic PCR in Droplets: Advances, Challenges and Future[J]. Analytica Chimica Acta, 2016, 914:7-16.

[12] Jacobs B K, Goetghebeur E, Clement L. Impact of variance components on reliability of absolute quantification using digital PCR[J]. Bmc Bioinformatics, 2014, 15(1):3419-3420.

[13]Pohl G, Iem S. Principle and applications of digital PCR.[J]. Expert Review of Molecular Diagnostics, 2004, 4(1):41-7.

[14] Bian X, Jing F, Gang L, et al. A microfluidic droplet digital PCR for simultaneous detection of pathogenic Escherichia coli, O157 and Listeria monocytogenes[J]. Biosensors & Bioelectronics, 2015, 74:770-777.

[15] Wang P, Jing F, Li G, et al. Absolute quantification of lung cancer related microRNA by droplet digital PCR[J]. Biosensors & Bioelectronics, 2015, 74:836-842.

[16] Becker T A, Kipke D R, Brandon T. Calcium alginate gel: A biocompatible and mechanically stable polymer for endovascular embolization[J]. Journal of Biomedical Materials Research, 2001, 54(1):76-86.

[17] Tan W H, Takeuchi S. A trap-and-release integrated microfluidic system for dynamic microarray applications.[J]. Proceedings of the National Academy of Sciences of the United States of America, 2007, 104(4):1146-1151.

CONTACT

*Linfen Yu, Tel: +86-18588466169; linfen.yu@hotmail.com

*Tianzhun Wu, Tel: +86-755-86392339; tz.wu@siat.ac.cn